Functional sensitivity of Multiband Echo-planar imaging in subcortical region

Author

Azmat Ullah

Registration Number

00000172097

Supervisor

Dr. Syed Omer Gilani

DEPARTMENT OF BIOMEDICAL ENGINEERING

SCHOOL OF MECHANICAL & MANUFACTURING ENGINEERING

NATIONAL UNIVERSITY OF SCIENCES AND TECHNOLOGY

ISLAMABAD

FABRUARY 12, 2019

Functional sensitivity of Multiband Echo-planar imaging in subcortical region

Author

Azmat Ullah

Registration Number

00000172097

A thesis submitted in partial fulfillment of the requirements for the degree of

MS Biomedical Engineering

Thesis Supervisor:

Dr. Syed Omer Gilani

Thesis Supervisor's Signature: _____

DEPARTMENT OF BIOMEDICAL ENGINEERING

SCHOOL OF MECHANICAL & MANUFACTURING ENGINEERING

NATIONAL UNIVERSITY OF SCIENCES AND TECHNOLOGY,

ISLAMABAD

FABRUARY 12, 2019

Thesis Acceptance Certificate

It is certified that MS thesis written by Azmat Ullah (Registration No. 00000172097), of SMME (School of Medical & Manufacturing Engineering) has been vetted by undersigned, found complete in all aspects as per NUST statutes/ regulations, is free of plagiarism, errors and mistakes and is accepted as partial fulfillment for award of MS/MPhil Degree. It is further certified that necessary amendments as pointed out by GEC members of the scholar have also been incorporated in this dissertation.

Signature:
_____
Name of Supervisor: Dr. Syed Omer Gilani
Date: _____

Signature (HOD): _____
Date: _____

Signature (Principal): _____
Date: _____

MASTER THESIS WORK

We hereby recommend that the dissertation prepared under our supervision by: (Student Name & Regn No) **Azmat Ullah** Reg no. **00000172097**

Titled: **Functional sensitivity of Multiband Echo-planar imaging in subcortical region** be accepted in partial fulfillment of the requirements for the award of **MS Biomedical Engineering** degree. (Grade _____)

Examination Committee Members

Name: **Dr. Adeeb Shehzad** Signature:_____

Name: **Dr. Umer Ansari** Signature:_____

Supervisor's name: **Dr. Syed Omer Gilani** Signature:_____

Date:_____

_____ _____

Head of Department Date

COUNTERSINGED

Date:_____ Dean/Principal_____

Declaration

I certify that this research work titled "*Functional sensitivity of Multiband Echo-planar imaging in subcortical region"* is my own work. The work has not been presented elsewhere for assessment. The material that has been used from other sources it has been properly acknowledged / referred.

Signature of Student

Azmat Ullah

Registration #: 00000172097

Plagiarism Certificate (Turnitin Report)

This thesis has been checked for Plagiarism. Turnitin report endorsed by Supervisor is attached.

Signature of Student
Azmat Ullah

Registration Number: 00000172097

Signature of Supervisor
Dr. Syed Omer Gilani

Proposed Certificate for Plagiarism

It is certified that PhD/M.Phil. /MS Thesis Titled by **Functional sensitivity of multiband echo-planar imaging in subcortical region** has been examined by us. We undertake the follows:

a. Thesis has significant new work/knowledge as compared already published or are under consideration to be published elsewhere. No sentence, equation, diagram, table, paragraph or section has been copied verbatim from previous work unless it is placed under quotation marks and duly referenced.

b. The work presented is original and own work of the author (i.e. there is no plagiarism). No ideas, processes, results or words of others have been presented as Author own work.

c. There is no fabrication of data or results which have been compiled/analyzed.

d. There is no falsification by manipulating research materials, equipment or processes, or changing or omitting data or results such that the research is not accurately represented in the research record.

e. The thesis has been checked using TURNITIN (copy of originality report attached) and found within limits as per HEC plagiarism Policy and instructions issued from time to time.

Name & Signature of Supervisor
Dr. Syed Omer Gilani
Signature: _____

Copyright Statement

- Copyright in text of this thesis rests with the student author. Copies (by any process) either in full, or of extracts, may be made only in accordance with instructions given by the author and lodged in the Library of NUST School of Mechanical & Manufacturing Engineering (SMME). Details may be obtained by the Librarian. This page must form part of any such copies made. Further copies (by any process) may not be made without the permission (in writing) of the author.

- The ownership of any intellectual property rights which may be described in this thesis is vested in NUST School of Mechanical & Manufacturing Engineering, subject to any prior agreement to the contrary, and may not be made available for use by third parties without the written permission of the SMME, which will prescribe the terms and conditions of any such agreement.

- Further information on the conditions under which disclosures and exploitation may take place is available from the Library of NUST School of Mechanical & Manufacturing Engineering, Islamabad.

Acknowledgements

I am thankful to my Creator Allah Subhana-Watala to have guided me throughout this work at every step and for every new thought which You setup in my mind to improve it. Indeed I could have done nothing without Your priceless help and guidance. Whosoever helped me throughout the course of my thesis, whether my parents or any other individual was Your will, so indeed none be worthy of praise but You.

I am profusely thankful to my beloved parents who raised me when I was not capable of walking and continued to support me throughout in every department of my life.

I would also like to express special thanks to my supervisor Dr. Syed Omer Gilani for his help throughout my thesis and also for Biomedical Image analysis course which he has taught me. I can safely say that I haven't learned any other engineering subject in such depth than the ones which he has taught.

I would also like to pay special thanks to Dr. Nabeel Anwar for his tremendous support and cooperation. Each time I got stuck in something, he came up with the solution. Without his help I wouldn't have been able to complete my thesis. I appreciate his patience and guidance throughout the whole thesis.

I would also like to thank Miss Zahra Fazal, Dr. Umar Ansari and Dr. Adeeb Shehzad for being on my thesis guidance and evaluation committee and express my special thanks to Miss Zahra Fazal for her tremendous help.

I would like to thank Amna Malik for her guidance and help throughout my research and my fellow lab members including Atif Sultan, Ahmed, Saad Habib Qureshi, Sarosh Bilal, Maliha Asad Khan, Sonia Malik, Zaeem, Azeem, Aftab Ullah Khan, Sheikh Arslan Waqar and Ahmed Shubahni.

Dedicated to my exceptional parents and adored siblings whose tremendous support and cooperation led me to this wonderful accomplishment.

Abstract

Functional magnetic resonance imaging (fMRI) is widely used technique for Brain functional connectivity analysis. MRI Acquisition acceleration is a hot area of research from many decades where a number of techniques were suggested. Echo planar imaging (EPI) is one of the most promising acceleration techniques in most fMRI studies. However, advancement to shorten the acquisition time using EPI have been proposed recently and simultaneous multi slice imaging technique is one of the most promising technique allowing acquisition of multiple slices simultaneously yielding an equivalent reduction of time. This technique has recently been using in resting state fMRI studies along with dual regression for group comparison. While the benefit of acquisition time reduction by high multiband acceleration factor (M) appears tempting, sensitivity of resting state network in subcortical region have only been investigated partially. In this study, we therefore used resting state fMRI data of 18 subjects acquired with two different multiband acceleration factors (M=1 and M=4), to investigate sensitivity of default mode network in datasets with increasing acceleration factor. Our results suggest that there is no significant sensitivity difference between common default mode network got from data acquired with both the acceleration factor.

Key Words: *Resting State fMRI, Default Mode Network, Echo planer imaging, Multiband Echo planer imaging*

Table of Contents

1 INTRODUCTION 1

1.1 Resting state fMRI 4

1.2 Resting state networks 5

1.3 Multiband Echo planer imaging 8

1.4 Independent component analysis 11

2 LITERATURE REVIEW 13

3 METHODOLOGY 16

3.1 Data Description 16

3.2 Pre processing 17

3.3 Conventional preprocessing 17

3.3.1 Brain Extraction 18

3.3.2 Slice time correction 19

3.3.3 Spatial smoothing 21

3.3.4 Temporal filtering 23

3.3.5 Registration 25

3.4 Nuisance Regression 28

3.4.1 ICA clean up 28

3.5 Group level ICA 30

3.6 Dual regression 31

3.7 Randomise 34

4 RESULTS 37

4.1 Statistical Analysis 38

List of Figures

Figure 1.1: The BOLD signal is an indirect measure of neuronal activity that is mediated by a slow increase in local oxygenated blood flow that takes several seconds to peak. (a) Several complex biological processes such as neurovascular coupling take place, which together result in the localized increases in blood oxygenation that are measured in BOLD fMRI. (b) The standard form of the hemodynamic response function is shown. From stimulus onset, the BOLD signal takes approximately 5 seconds to reach its maximum.....2

Figure 1.2: Resting state networks and consciousness Alterations of multiple resting state network connectivity in physiological, pharmacological, and pathological consciousness states Lizette Heine et al.....7

Figure 1.3: Using a multiband EPI sequence allows us to push the limits of spatial and temporal resolution. In multiband EPI, data are acquired from multiple slices at once, the multiband factor describes the number of slices acquired at the same time (here the MB factor is six). As described previously, the 16-degree tilt of the field of view helps ensure full brain coverage in a large percentage of the population.....9

Figure 3.1: Brain extraction of structural scan 18

Figure 3.2: Brain extraction of functional scan (A) functional scan with skull (B) skull stripped functional scan (C) skull stripped structural scan overlaid over raw structural scan 19

Figure 3.3: Slice time correction.....21

Figure 3.4: Left: no spatial smoothing, Right: spatial smoothing of 6mm 22

Figure 3.5: Effects of temporal filtering. The raw BOLD signal (extracted from the posterior cingulate cortex) shown on the top displays some drift (i.e., the signal amplitude slowly goes up over time). After high-pass filtering this drift has been removed from the data, as shown in the graph in the middle (i.e., the signal at the start of the sequence is no longer lower than the signal at the end of the sequence). On the bottom, the effects of bandpass filtering are shown. Bandpass filtering removes both low and high frequencies from the data, resulting in a smoother timecourse.....24

Figure 3.6: Depiction of location differences if the data is not co-registered 25

Figure 3.7: Registration methods are used to put data from different subjects into the same space so that group comparison can be performed. (a) Different images are acquired in different "spaces." This illustrates a two-stage registration process. (b) The first stage of registration involves estimating the required transformations (which can either be linear matrices, or non-linear warp images). (c) The second step of registration involves applying the transformation in order

TO RESAMPLE AN IMAGE INTO A DIFFERENT SPACE. THE TRANSFORMATIONS CAN BE COMBINED AND APPLIED TO RESAMPLE THE EPI FUNCTIONAL DATA INTO STANDARD SPACE. 26
FIGURE 3.8: DUAL REGRESSION IS A TWO-STAGE PROCESS AIMED AT OBTAINING COMPONENT SPATIAL MAPS FOR EVERY SUBJECT. THE DATA INPUT TO THE MULTIPLE REGRESSION ANALYSIS IS THE SAME IN BOTH STAGES (I.E., THE PREPROCESSED BOLD DATA FROM ONE SUBJECT). THE MODEL INPUT FOR STAGE 1 CONTAINS THE SET OF ICA COMPONENTS FROM THE GROUP-ICA. THE OUTPUTS OF STAGE 1 ARE THE SUBJECT-SPECIFIC COMPONENT TIMESERIES FOR EACH GROUP COMPONENT OF INTEREST, AND THESE ARE USED AS THE MODEL INPUT FOR STAGE 2 OF THE DUAL REGRESSION ANALYSIS. THE SPATIAL MAPS THAT ARE OBTAINED FROM STAGE 2 CAN BE USED IN A GROUP ANALYSIS. 33
FIGURE 4.1: THE HEATMAP SHOWN IN THIS FIGURE IS THE Z- STATISTICS VALUES. (A) IS THE GROUP COMPARISON RESULT WHERE THERE IS NO PIXEL SHOWING SIGNIFICANT DIFFERENCE. (B) MAP SHWON IN THIS FIGURE IS THE Z-VALUES OF INDEPANDENT SAMPLE T-TEST RESULT. (C) MAP SHWON IN THIS FIGURE IS THE Z-VALUES OF INDEPANDENT SAMPLE T-TEST RESULT. 38
FIGURE 4.2: SHAPIRO WILK TEST RESULT, SHOWING THAT THE DATA DISTRIBUTION OF BOTH THE GROUPS ARE NORMAL. 39
FIGURE 4.3: BOX-PLOT OF NUMBER OF VOXEL IN EACH GROUP 40

1 INTRODUCTION

On a general level, there are two overarching concepts in the field of neuroimaging that can inform us about how the brain works. The first of these is *localization*, which aims to assign functions to specific regions of the brain. Many researchers use carefully designed behavioral tasks that subjects perform in the MRI scanner in order to localize functionally specialized regions of the brain that activate in response to a specific aspect of behavior. Tasks typically include multiple different conditions (including baseline periods), and task-induced activation is measured and localized by comparing the blood oxygen level dependent (BOLD) signal between different conditions. The second general concept is to investigate *connectivity*, or the way in which brain regions communicate with one another and information is passed from one brain area to the next. In order to investigate connectivity, we measure the similarity of the BOLD signals from different brain regions, because if the signals are similar, this is likely to mean that the regions are passing on information from one region to the other (i.e., there is connectivity). In order to study connectivity, we often look at spontaneous fluctuations in the signal, when there are no specific cognitive demands for the subject (so-called resting state scans). Using spontaneous fluctuations allows us to investigate similarity between regions when it is not biased by any specific task. As such, resting state fMRI has emerged as a valuable way to study brain connectivity. It is useful to understand how these concepts relate to physiological processes in the brain both at the neuronal level and at the macroscopic level that we measure in fMRI (Figure 1.1). At the microscopic level, a neuron consists of a cell body (soma) that receives input through dendrites and passes action potentials through axonal tracts

to other cells. These microscopic processes in turn result in a localized increase in blood flow that far exceeds the oxygen demands of the neural activity, leading to a local increase in blood oxygenation level (Figure 1.1). It is crucial to appreciate that BOLD fMRI measures this increase in blood oxygenation, which is a secondary and indirect measure of neuronal activity. The hemodynamic response to neural activity which is measured in fMRI (i.e., blood oxygenation levels) is a relatively slow process that only reaches its peak approximately 5–6 seconds after the start of the neural activity. Using concurrent fMRI and electrophysiological recording, previous research has shown a strong link between spontaneous fluctuations in resting state BOLD data and slow fluctuations in the local field potential (LFP). Therefore, the BOLD signal is thought to primarily reflect the excitatory inputs to the neural population (synchronized post-synaptic activity).

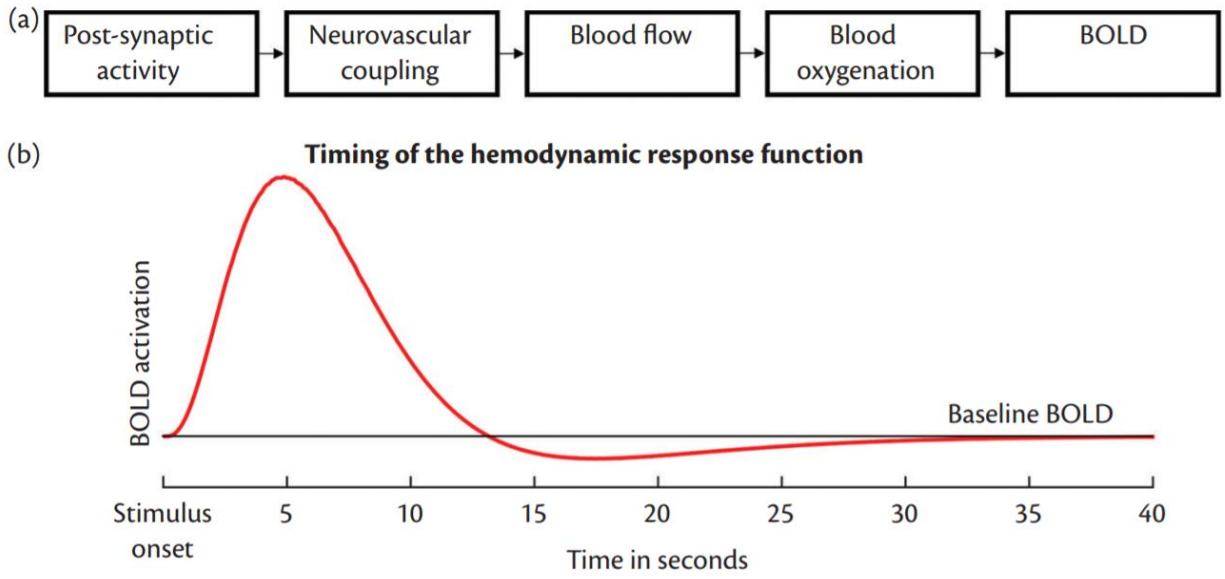

Figure 1.1: The BOLD signal is an indirect measure of neuronal activity that is mediated by a slow increase in local oxygenated blood flow that takes several seconds to peak. (a) Several complex

biological processes such as neurovascular coupling take place, which together result in the localized increases in blood oxygenation that are measured in BOLD fMRI. (b) The standard form of the hemodynamic response function is shown. From stimulus onset, the BOLD signal takes approximately 5 seconds to reach its maximum

Functional connectivity is typically defined as: "the observed temporal correlation (or other statistical dependencies) between two electro- or neurophysiological measurements from different parts of the brain." For resting state fMRI this definition means that functional connectivity can inform us about the relationship between BOLD signals obtained from two separate regions of the brain. The underlying assumption is that if two regions show similarities in their BOLD signals over time, they are functionally connected.

The simplest way to investigate similarity between two signals is by looking at their timeseries *correlation* using Pearson's correlation coefficient. Correlation ranges from –1 (perfect negative correlation) to +1 (perfect positive correlation), where 0 indicates no relationship on average between two signals. In 1995, Biswal and colleagues compared task activation maps during finger tapping with a map of correlation coefficients of BOLD data obtained during a scan when the subject was resting. The resting state correlation map was created by taking all voxels that were activated by the motor task and using only the resting state data to calculate the correlation of each voxel in the brain with those "activated" voxels. The task activation map and resulting resting state correlation map showed strong spatial similarities. This work is now often cited as the first study to show that intrinsic fluctuations measured in the brain at rest by functional MRI hold information about the inherent functional organization of the human brain. The spatial structure of functionally

connected regions, which is consistently and reliably found in resting state fMRI data, forms the foundation for resting state fMRI research. Therefore, while functional connectivity is defined in terms of temporal similarity between signals, the spatial patterns that emerge when looking at connectivity are often of primary interest in functional connectivity research.

1.1 Resting state fMRI

Resting state fMRI is aimed to detect low frequency (<0.1Hz), spontaneous fluctuations in BOLD signal. For the first time Biswal in his study in 1995 have documented the functional importance of these fluctuations[1]. In his study, he instructed the subjects to not perform any motor or cognitive task. The author demonstrated high correlation of low frequency fluctuations in BOLD signal between bilateral somatosensory cortexes in subjects at rest. Similar synchronous fluctuations were also noted in visual and auditory cortex, identifying all of these to be indicators of functional connectivity of brain.

Resting state fMRI is identical to conventional fMRI, however it does not need the subject to respond to a stimulus or perform an explicit task. BOLD data of whole brain is collected while the subject lie in the scanner with staring at fixed point or their eyes closed. Normally T2-weighted echo-planar images are acquired with isotropic spatial resolution of 3-4 mm, TR values of 2-3 sec, and if available, with multi-band acceleration.

1.2 Resting state networks

With resting state fMRI, at least 10 distinct maps of brain connections called resting state networks (RSNs) were discovered. The most significant RSNs include visual and auditory processing network, salience, dorsal attention, executive control and default mode network (most active network at rest, containing posterior cingulate and superior parietal areas involved in attention and consciousness) [2]. These networks have provided important understandings into the cognitive organization of the brain in health and disease.

A group or system of interconnected people or things is often called a network. Think, for example, about your social media network or a computer network. Given the definition of functional connectivity described above, a *resting state network* is simply a set of brain regions that show similarities in their BOLD timeseries obtained during rest. At present, we do not have a complete understanding of the network structure of the resting brain. Nonetheless, several networks can be reproducibly found using a variety of analysis approaches. Different resting state networks have been identified and "named" mostly on the basis of the spatial similarity between the resting state networks and activation patterns seen in task fMRI experiments. This naming convention is most accurate for areas associated with sensory processing, where it has been established that a correspondence exists between areas that can be mapped in response to sensory stimulation and areas that have strong resting state BOLD similarities. Other parts of the brain, for example within multimodal association cortex, are more ambiguously related to task experiments. Perhaps the best-known resting state network of all is the *Default Mode Network* (DMN; Figure 1.2). The DMN contains regions in the brain that

consistently show decreases in activity when the brain is performing any type of task compared with rest (*deactivations*), as shown by early task-based imaging studies using both fMRI and positron emission tomography (PET). Key regions of the DMN are the posterior cingulate cortex, precuneus, medial prefrontal cortex, inferior parietal lobule, and lateral temporal cortex. The *dorsal attention network* (DAN; also called the task-positive network; Figure 1.2) is another commonly described network made up of regions that are commonly activated during various types of goal-directed behavior. Regions that are included in the DAN are the inferior parietal cortex, frontal eye fields, supplementary motor area, insula and dorsolateral prefrontal cortices. Some findings suggest that the DMN and the DAN may be anticorrelated, although these results may, in part, be driven by preprocessing choices. Other commonly described networks include multiple distinguishable visual networks (including dorsal and ventral visual networks), auditory networks, and sensorimotor networks. In addition to the DMN and DAN, additional cognitive networks include salience, executive control, and fronto-parietal networks. It is important to note that this nomenclature describes a categorization of the brain at a single and somewhat arbitrarily chosen level of granularity. This is to say that these resting state networks form a hierarchy, where networks can be broken down further into yet finer-grained systems (i.e., form "networks within networks"). As such, it is not the case that every area in the brain can be uniquely assigned to one of a set of resting state networks. Indeed, brain regions that are known to

have extensive connectivity with many other brain regions, also show functional connectivity with multiple resting state networks.

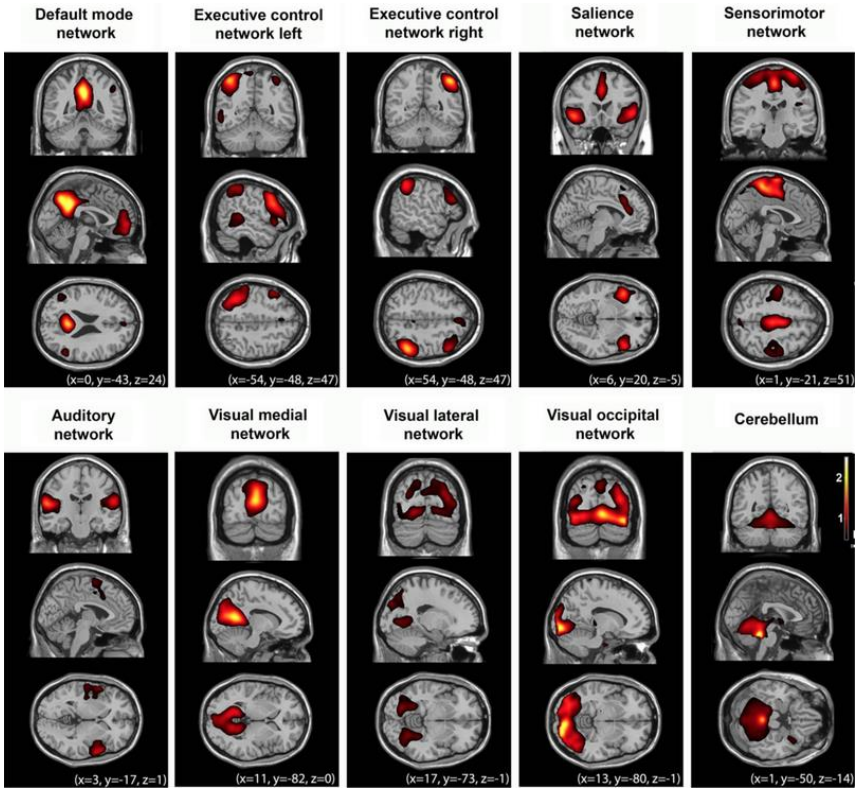

Figure 1.2: Resting state networks and consciousness Alterations of multiple resting state network connectivity in physiological, pharmacological, and pathological consciousness states Lizette Heine et al.

1.3 Multiband Echo planer imaging

Multiband (MB) echo planer imaging is a technique in which a complex radio frequency pulse along with parallel imaging is used to scan multiple slices at a time. It is also known as simultaneous multi-slice (SMS) imaging technique.

For the first time (Larkman et al, 2001) used multi-band (MB) imaging with a spine radio frequency coil and leg imaging [3]. In the MB approach, a specific excitation pulse is used to excite each slice at the same time, and multiple coils are placed which are tuned to sense a specific frequency in parallel to the other coils. These slices are unaliased after the multiple slice acquisition is done. In brain imaging Nunes et al (2006) was the first to introduce the application of Multiband to echo planer imaging [4]. In 2012 Uğurbil et al, studied the possibility of using Multiband imaging to acquire high resolution functional brain images at 7 T over the entire brain [5].

In typical echo planar imaging (EPI), data are acquired slice-by-slice, meaning that the data are acquired from one thin slab of the brain, before moving on to the next slab. Modern MRI equipment allows for signals from multiple detector coils to be measured simultaneously. When using a multiband (or simultaneous multislice) accelerated sequence, multiple slices of the brain are acquired at the same time and information from multiple radiofrequency coils is used in order to separate the overlapping images into their separate slices. In order to separate signals from different slices, a multi-channel radiofrequency coil, with at least 32 channels, is necessary. The number of slices that are acquired at the same time in a multiband EPI sequence is known as the multiband factor, and this factor controls the amount of speed-up that is obtained. While the trade-off between spatial and temporal resolution is still there when using a multiband sequence, it is

much less limiting due to the parallel acquisition of multiple slices. For example, it is possible to acquire whole-brain data at 2 mm isotropic spatial resolution with a TR of roughly 1 second when adopting a multiband factor of 6–8 (i.e., acquiring 6 or 8 slices at the same time). In contrast, a typical whole-brain non-multiband EPI acquisition is likely to have 2.5–3.5 mm isotropic voxels and a TR of approximately 3 seconds.

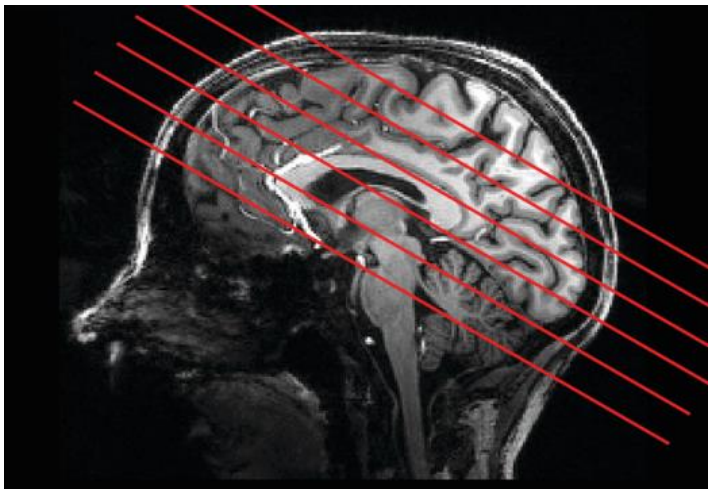

Figure 1.3: Using a multiband EPI sequence allows us to push the limits of spatial and temporal resolution. In multiband EPI, data are acquired from multiple slices at once, the multiband factor describes the number of slices acquired at the same time (here the MB factor is six). As described previously, the 16-degree tilt of the field of view helps ensure full brain coverage in a large percentage of the population.

Multiband EPI sequences can be used to reduce the voxel size, and/or the TR compared with non-multiband EPI. Researchers typically choose parameters such that the biggest benefit of the multiband acquisition is the reduction in the TR (due to the downsides of extremely small voxel sizes discussed above). There are two main benefits of reducing the TR. The first is that a shorter TR allows sampling of a wider range of frequencies, which improves the sampling of the signal, and can also help with preprocessing, if the TR is fast enough to sample key periodic signals, such

as the respiratory cycle. The second advantage of a shorter TR is that increasing the total number of time points in the resting state dataset improves the statistical power in analyses because it increases the temporal degrees of freedom.

Despite the improvement in spatio-temporal resolution achieved when using a multiband EPI sequence, there are some important differences between regular EPI and multiband EPI data. First, multiband data can suffer from more artifacts compared with non-multiband EPI.

In addition, artifacts that are common to regular and multiband EPI can often look different in multiband EPI due to the multislice acquisition. An example of this is head motion, which can show up as a striped pattern (one line along each simultaneously acquired slice) in multiband EPI, due to the interaction between motion and the slice acquisition pattern. A further effect of multiband EPI acquisition is that the tissue contrast between gray and white matter can be much lower than it is in non-multiband EPI. This reduction in tissue contrast occurs when using short TRs, because the slices are excited in rapid succession, giving tissue less recovery time. Due to these differences in terms of data acquisition and artifacts, there are some implications for the analysis of multiband data. To address the reduced tissue contrast, it is important to make sure that the sequence also writes out a single-band reference image (a single fMRI volume, often called "SBref"). The purpose of this image is primarily to calibrate the coil profiles to help in the separation of concurrently acquired slices, but this SBref image also has good tissue contrast. The SBref image can subsequently be used for motion correction and for registration to make sure the lack of tissue contrast in the rest of the functional images does not affect these important preprocessing steps. Secondly, due to the sensitivity of multiband EPI to distortions, it is important

to apply appropriate shimming during acquisition, and to acquire fildmaps that can be used later to correct for distortions and aid registration. Finally, head motion can interact with the multi-slice acquisition in multiband data causing striping artifacts, as explained previously. Therefore, it is particularly important to make sure this potential source of noise is dealt with appropriately when preprocessing the data.

1.4 Independent component analysis

Independent component analysis (ICA) is a statistical and computational technique separating unknown sources that underlie sets of signals, measurements, or random variables. ICA is a data driven technique which outlines a generative model for the observed multivariate data, which is typically given as a large database of samples. To decompose the data into its components, the data must be a linear mixture of some unknown source components, and the mixing mechanism of these components is also unknown. The source variables are supposed to be non-gaussian and independent of each other. These independent components combine to form the data that is why their separation method is called independent component analysis.

There exist other methods for source separation, such as principal component analysis and factor analysis, but ICA is superficial related to these techniques, and is much more powerful and capable of finding unknown sources and factors concealed in the data when the other classic methods fail completely.

The data input for ICA can come from many kinds of sources including time series data, digital image data or psychometric measurements. This data in many cases is in the form of time

series or a set of parallel signals; the term blind source separation is used to characterize this problem. Typical examples of input data are mixtures of electroencephalogram signals recorded by multiple sensors, interfering radio signals arriving at the mobile phone, BOLD signal of a brain functional magnetic resonance imaging, simultaneous speech signals that have been picked up by several microphones or parallel time series obtained from some industrial process.

2 LITERATURE REVIEW

Functional magnetic resonance imaging (fMRI) is widely used technique for Brain functional connectivity analysis. Predominantly, the resting state networks obtained from fMRI is based on the correlation of Blood Oxygenation Level Dependent (BOLD) Signal [6,7]. At this time the most widely used acquisition technique is echo planar imaging (EPI) [8] with its high acquisition acceleration, and high sensitivity towards BOLD signal, is mainly used in almost every fMRI study [9,10]. Repetition Time (TR) of several seconds is required to acquire whole brain image. Recent advancement in fMRI acquisition protocols [11], parallel imaging [12,14] and sparse sampling technique [15,17] has empowered to accelerate the acquisition speed to a considerable factor, with full brain coverage at acquisition time of about one to two seconds. Although, parallel imaging is relatively very fast, but we are still not be able to completely understand the temporal and spatial characteristics of large-scale brain networks. Reduction in scan time by this technique has significant effect on SNR due to the fact that high acceleration factor shortens the echo train resulting in a lesser amount of echo time. A typical sensitivity to bold signal requires the echo time to be nearly equal to the repetition time TR. An echo time of 30ms to 40ms is most commonly used in majority of the fMRI studies at 3T due to the critical signal loss in areas with strong background susceptibility gradients as in orbitofrontal and temporal areas of the brain and SNR reduction at longer echo times. Although T2 of 50ms was found in most of the areas of brain [18].

Multiband Echo planar or simultaneous multi slice (SMS) is an alternative technique [19] used to decrease acquisition time considerably without effecting the echo time and hence not

decreasing SNR by scanning of multiple slices simultaneously. Like parallel imaging, spatial encoding in multiband imaging relies critically on the varying sensitivities of RF receive coil arrays. Multiple slices can be excited simultaneously by multiband RF pulses [20,21]. These slices can be reconstructed easily through SENSE algorithm [22]. Multiband echo planar imaging considerably reduces acquisition time by simultaneously exciting multiple slices, i.e. the multiband factor (M). Due to a reduced number of sampling with acceleration factor of R, parallel imaging is a good way to preserve the spatial information of acquired data but in consequence the SNR of the data is decreased. Though, with increasing M-factor the amplification of spatially dependent noise may increase depending on coil geometry, which can be quantified by a geometry factor g [23].

In human brain studies, multiband echo planar imaging was first demonstrated by Nunes et al [3]. Due to small distance space between the simultaneously excited slices they found a strong noise amplification which was causing ill-natured unaliasing problem. To alleviate this, a wideband technique [24] was used where they introduce a shift between pixels in phase encoding direction by means of unipolar blips in slice direction. This technique helped reduce unaliasing, but also resulted in blurring effect due to the effective voxel tilt. This technique is recently extended by Setsompop et al. by introducing ‘blipped-CAIPI’ where balanced gradient blips in slice direction to achieve alternating phase shifts similar to 'controlled aliasing in parallel imaging results in higher acceleration' (CAIPIRINHA) [25,26]. Xu et al. in their study concluded that multiband factor of up to 8 can be used without any aliasing when blipped CAIPI is employed [27]. They have compared signal leakage between simultaneously excited slices and noise enhancement in a systematic way in multiband echo planar imaging using acceleration factor of

up to twelve. Simultaneous multi slice imaging has also been used in combination with simultaneous echo refocusing and parallel imaging [28,29,30]. Generally, multiband echo planar imaging is now mature enough to be used on a broader scale. A number of studies show that these acceleration techniques have enhanced the capabilities of task as well as resting state fMRI [31,32].

3 METHODOLOGY**Data Description**

The resting state fMRI data used in this research is from "1000 functional connectomes project", containing data of more than 1200 subjects and is independently collected at more than 33 sites around the globe. The dataset consists of resting state data of 18 subjects in 2 sessions with a TR of 645ms (M4) and 2500ms (M1) respectively. The first session was acquired at a multiband factor of 4 with voxel size of 3x3x3mm, 960 volumes and at a total run time of 10 minutes. The second session was acquired at a multiband factor of 1 with voxel size of 3x3x3mm, 120 volumes and at a total run time of 5 minutes. The flip angles used for group 1 and 2 was 60 and 80 respectively. These flip angles were adjusted to have signal strength as maximum as possible. The M4 dataset was truncated to have the acquisition time similar to that of the M1 dataset. It is reported by Van Dijk and colleagues that a scan time of 5 minute is enough to detect resting state networks easily.

For satisfactory registration of functional scan to standard space, T1- weighted scan was also acquired for each subject. The voxel size of structural scan was 2mm isotropic, with FOV of 256 and 36 number of slices.

Group	1	2
No. of Subjects	18	18
Repetition Time (TR)	645ms	2500ms
Multiband Factor	4	1
Sampling	Interleaved	Interleaved
Voxel Size	3x3x3	3x3x3
No. of time points	480	120
Acquisition Time	5 Minutes	1 Minutes

3.2 Pre processing

For every fMRI analysis the first step is to preprocess the data. For preprocessing FMRIB Software Library (FSL) was used. The preprocessing was done in two steps, Conventional preprocessing and Noise reduction, which are discussed in detail in the following sections.

3.3 Conventional preprocessing

The common preprocessing steps involved in conventional preprocessing are as follows

3.3.1 Brain Extraction

FSL bet tool was used to remove unwanted tissues like skull and fat. Fractional Intensity Threshold (FIT) parameter is used to control the overall segmentation of brain. Default value of FIT is 0.5 and should be in the range of 0-1. FIT of <5 segment the brain region larger while FIT of >5 segment the brain region smaller.

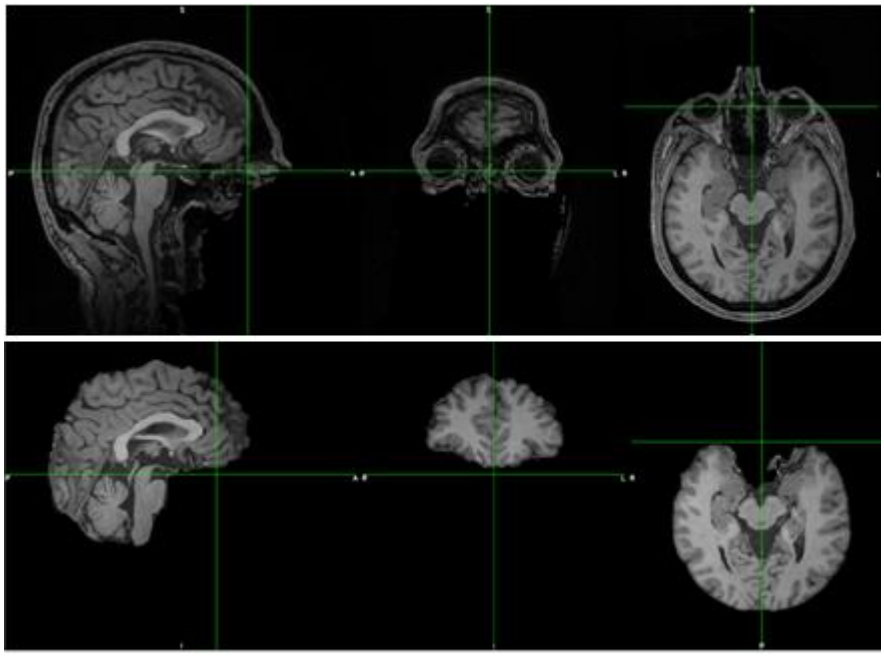

Figure 3.1: Brain extraction of structural scan

A brain mask was also generated and both T1-weighted and functional scan was brain extracted. Figure 3.1 shows T1-weigted scan with non- brain tissue. T1-weighted image has high resolution, so we used it as first step of brain extraction, a brain mask is generated which is used to extract brain in functional scan. A functional scan with non-brain tissue and skull stripped scan is shown in Figure 3.2. Figure 3.3 shows a binary brain mask overlaid on top of T1-weighted raw scan.

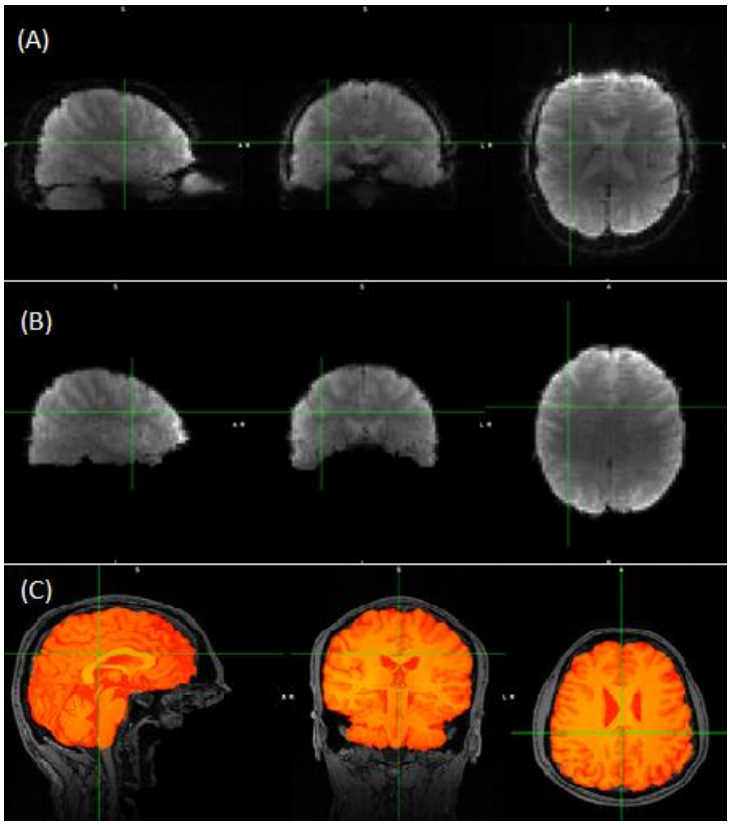

Figure 3.2: Brain extraction of functional scan (A) functional scan with skull (B) skull stripped functional scan (C) skull stripped structural scan overlaid over raw structural scan

3.3.2 Slice time correction

Data used in this research is acquired with slices being interleaved. Interleaved means that the sequence of slice acquisition is 1-3-5-7-2-4-6-8, this is because if the time required for whole volume acquisition is larger, there will be difference in BOLD signal at the first slice and at the last slice. Therefore, it is useful to apply slice time correction.

Figure 3.3 shows a depiction of slice time correction of interleaved data. Assuming the number of slices to be 8 and repetition time to be 2 seconds. The green colored slices were acquired first and then the red colored slices were acquired in 1 3 5 7 2 4 6 8 sequence. After slice time correction placement of each slice is corrected according to its position. The aim of this step is to correct for the slight difference in the time at which each slice of BOLD data was acquired (i.e., some slices are acquired at the start of the TR, whereas others are acquired later). When the TR of a sequence is, for example, 3 seconds, the difference in slice time acquisition can vary quite a lot and it may be useful to apply slice timing correction. However, with the development of accelerated multiband EPI sequences, the TR is often closer to 1 second or even less. Given the sluggishness of the hemodynamic response function, such small differences in slice time acquisition may have little effect on the analysis. Hence, in studies with fast TRs, it may be beneficial to avoid using slice timing correction because it also has disadvantages, such as the use of interpolation.

Slice timing correction uses interpolation in time to slightly shift the BOLD timecourses of voxels in order to account for these small differences in acquisition time. However, interpolation causes a slight temporal smoothing of the data, and therefore results in an unavoidable loss of high-frequency information. Finally, slice timing correction interacts with motion correction and spatial smoothing in ways that are complicated, and typically cannot be corrected fully.

Whether or not to apply slice timing correction should be determined separately for each individual study. This decision should be made based on the TR, and also on the aim of the study

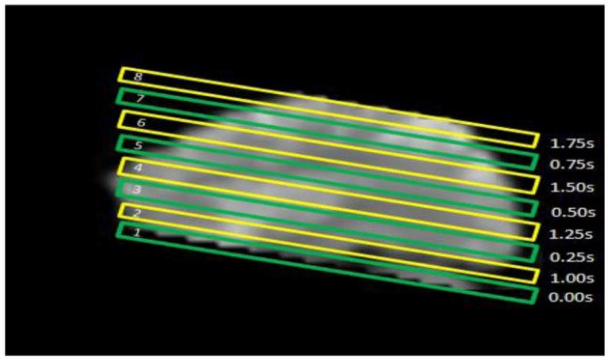

Figure 3.3: Slice time correction

and the type of analysis that will be performed after preprocessing (for example, in studies where exact timing is crucial to the hypotheses and methods, slice timing correction may become more important, even for fast TR data).

3.3.3 Spatial smoothing

The next step in conventional preprocessing is spatial filtering, which has the advantage of reducing noise. In this step a weighted average of certain numbers of neighboring voxels is calculated at each voxel. The amount of spatial smoothing is defined by Full Width Half Maximum (FWHM) of Gaussian kernel used to create weighting sum.

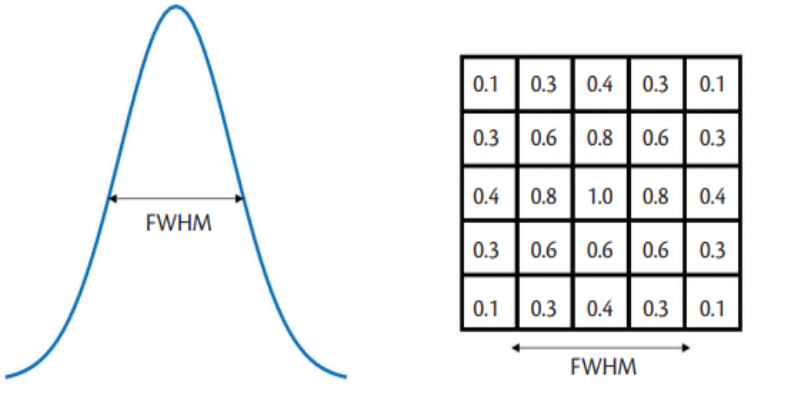

The value of FWHM is generally set to 1.5-2 times the size of voxel. So in our study the value of FWHM was set to 6mm. Figure 3.4 shows (A) a functional scan with no smoothing and (B) a functional scan with spatial smoothing of 6mm.

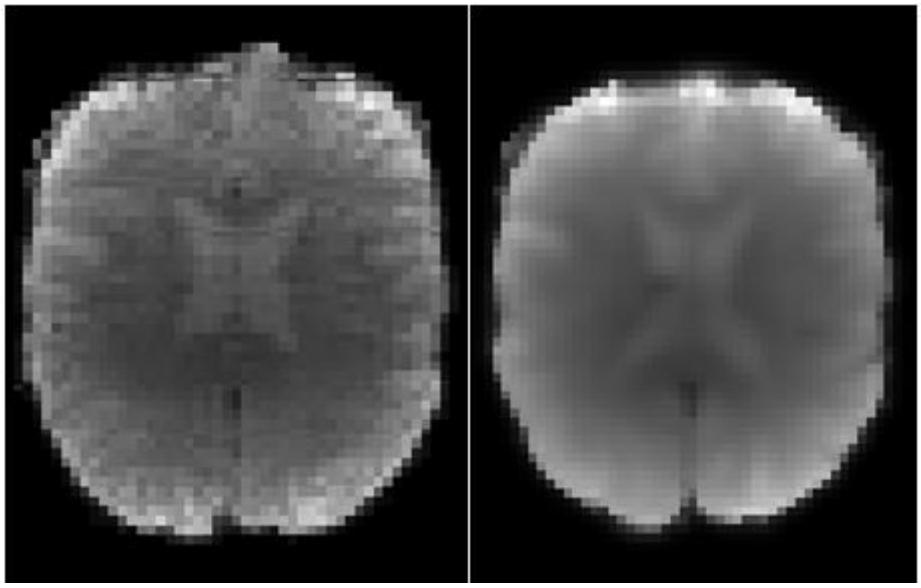

Figure 3.4: Left: no spatial smoothing, Right: spatial smoothing of 6mm

However, when deciding on the amount of smoothing to apply to the data, it is also important to consider the size of the regions that you are most interested in. For example, if the aim of a study is to investigate connectivity in the amygdala (a relatively small subcortical structure), then smoothing should be set smaller than the size of the amygdala. In this example,

applying too much smoothing would result in blurring the signal too much in the region that is of primary interest for the study.

In EPI datasets with high spatial resolution (i.e., equal to or less than 2.5 mm isotropic voxels) and high temporal resolution (i.e., TR below 1.5 seconds), as well as lengthy timeseries (i.e., at least 10 minutes of acquisition), smoothing is not always necessary. The reason for this is primarily related to the high number of timepoints available, because more time points leads to a higher number of degrees of freedom, which improves the ability to get accurate functional connectivity estimates. However, for lower resolution datasets (in particular, when the number of time points is relatively low), some degree of spatial smoothing may be advantageous.

3.3.4 Temporal filtering

Resting state networks are considered to have low signal fluctuations in the range of 0.01-0.1Hz. The fMRI data acquired initially has a lot of high frequency noise e.g. physiological and machine related noise. Therefore, the data is used to be band pass filtered. Figure 3.5 shows a time series of a single voxel which has both very low and high frequency fluctuations. If this time series is high pass filtered at frequency threshold of 0.01Hz, the linear trend is removed, and the signal fluctuates to a common baseline value.

Low pass filtering is not enough as the signal contains high frequency components, which is considered noise in resting state fMRI. So, a band pass filter is applied, which removed both low frequency fluctuations and high frequency noise. The low frequencies that we aim to remove here are ideally lower than the low-frequency fluctuations that dominate the BOLD signal. The amount of temporal filtering that is applied is typically expressed using a cut-off frequency or a cut-off period. For example, when a high-pass filter with a cut-off of 0.01Hz (or 100 seconds) is used, this means that any signal fluctuations that vary more slowly than the cut-off will be (entirely or

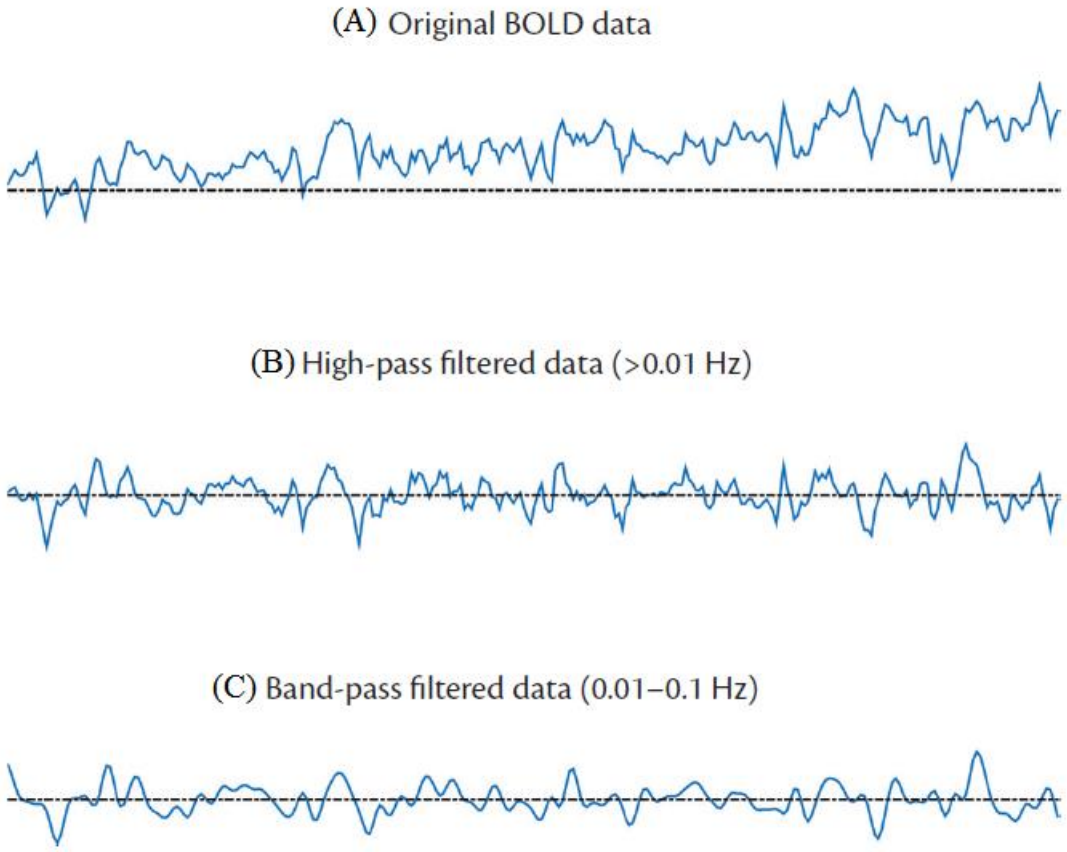

Figure 3.5: Effects of temporal filtering. The raw BOLD signal (extracted from the posterior cingulate cortex) shown on the top displays some drift (i.e., the signal amplitude slowly goes up over time). After high-pass filtering this drift has been removed from the data, as shown in the graph in the middle (i.e., the signal at the start of the sequence is no longer lower than the signal at the end of the sequence). On the bottom, the effects of bandpass filtering are shown. Bandpass filtering removes both low and high frequencies from the data, resulting in a smoother timecourse.

partially) removed Figure 3.5. Essentially, the aim of high-pass filtering is to remove scanner drift from the data (i.e., changes in the baseline of the BOLD signal that occur slowly over time as a result of the scanner hardware). It is typically advisable to apply high-pass filtering as part of preprocessing. The amount of filtering depends on the data quality; in high quality datasets it is possible to set a higher cut-off period (1000 seconds) in order to remove less and retain more data, whereas lower quality data often use lower cut-off periods (100 seconds) in order to remove more noise. In resting state fMRI, more stringent bandpass temporal filtering is sometimes applied.

3.3.5 Registration

For group analysis, each subject scan needs to be registered to a standard space. A standard space is a coordinate space used to standardize locations of different areas of brain. Montreal Neurological Institute (MNI) is a standard space template generated by taking MRI scans of large number of healthy subject brain. Another standard template used in MRI research is Talairach, which is created by taking photographs of dissected brain slices. The native space in which each subject data is acquired has different voxel size and dimensions, so a voxel in one

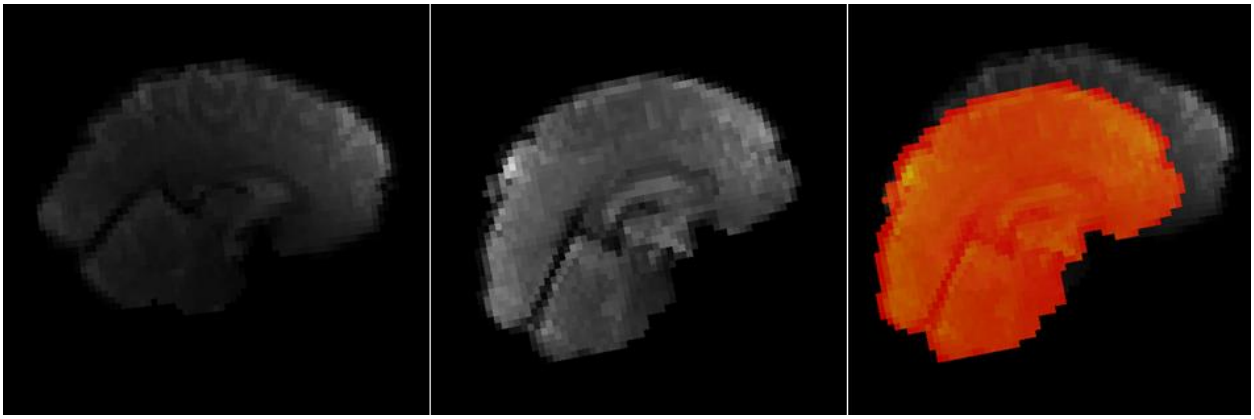

Figure 3.6: Depiction of location differences if the data is not co-registered

subject's scan will not cover the same area in the other subject's scan. So, the main purpose of registration is to match the spatial location of each subjects scan to standard scan.

In registration, first the functional scan is registered to the individual structural scan. In the next step, the individual structural scan is registered to standard space. A transformation matrix is generated for each step which can be used to transform from one space to another. An inverse transformation matrix can also be generated which can be used to transform back to previous space e.g. from standard space to individual structural space. This is also important, because if a region of interest is selected in standard space, it can be transformed easily into the individual functional

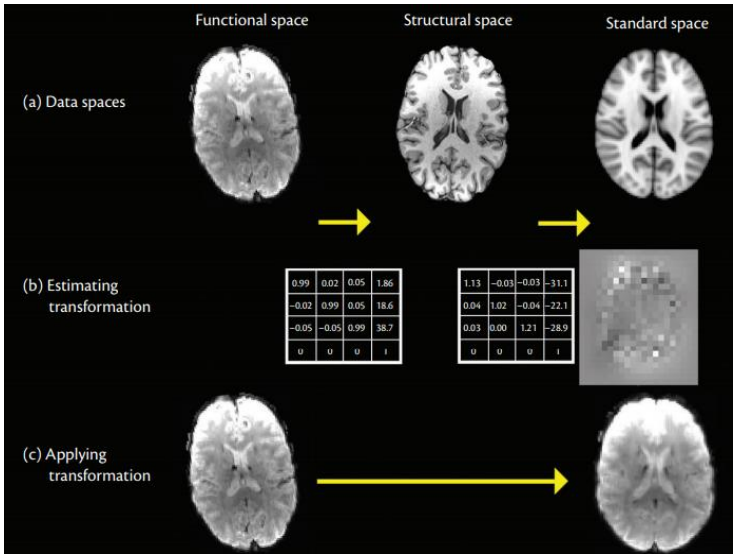

Figure 3.7: Registration methods are used to put data from different subjects into the same space so that group comparison can be performed. (a) Different images are acquired in different "spaces." This illustrates a two-stage registration process. (b) The first stage of registration involves estimating the required transformations (which can either be linear matrices, or non-linear warp images). (c) The second step of registration involves applying the transformation in order to resample an image into a different space. The transformations can be combined and applied to resample the EPI functional data into standard space.

scan using this transformation matrix.

Importantly, the brain can be represented in three-dimensional space as it exists in its natural form (also called volumetric space, made up of voxels). However, the gray matter cortex can also be represented on a surface made up of vertices. Registration can be performed in volumetric space or on the cortical surface. Without going into too much detail, the surface representation isolates the ribbon of gray matter that makes up the cortex and either represents this as a flattened sheet or inflates it until all the gyral folds flatten out, creating an inflated or spherical surface. There is general consensus that registration performed on a surface representation is superior for cortical regions, because in volumetric space two regions that lie on opposite sides of a sulcal fold would be right next to each other (because of the folding), whereas the surface would accurately reflect the biological distance between the same two regions (because they would separate as a result of flattening or inflation). It has been shown that much better cross-subject alignment of functional areas (and, hence, connectivity) can be achieved through surface-based registration, compared with volumetric registration. Additionally, it is beneficial to perform spatial smoothing on the cortical surface, rather than in volumetric space, to avoid blurring across the sulcal fold. However, surface representations do not capture all the subcortical regions, and these regions are known to play an important role in cognitive and clinical neuroscience. Therefore, it is necessary to work either in volumetric space, or to adopt a hybrid approach that represents the cortex on the surface and subcortical regions as volumes. Such a hybrid approach was developed as part of the Human Connectome Project in the form of a grayordinate system. A grayordinate is a gray matter location in the brain that is represented either by a surface vertex for cortical regions or by a volumetric voxel for subcortical regions.

3.4 Nuisance Regression

Nuisance Regression is commonly used to reduce the effect of structured noise in resting state fMRI. There are different versions of nuisance regression, which include physiological noise regression, global signal regression, volume censoring and Independent Component Analysis (ICA). In this research we used ICA for structured noise removal, which is discussed in detail in the following section.

3.4.1 ICA clean up

Unlike other model driven techniques for example Seed-based Correlation Analysis (SCA), ICA is a data driven technique used for blind source separation without the prior knowledge of the sources. ICA can be used to decompose the resting state fMRI data into a mixture of components. These components can either be a resting state network or a structured noise. Therefore, this approach is used for cleaning the resting state fMRI after identifying the noise components.

Conventionally pre-processed data of each subject is used when applying ICA for noise removal. These noise components are supposed to be extracted from the input data. For this we must identify which component is signal and which is noise. There are three criterions for the identification process of the components. We investigate the spatial location and its distribution of the map, as well as its time series and power spectra. The frequency components lying in the range 0-0.1 is signal, while other is noise.

Independent component analysis (ICA) is a method that can be used to decompose a whole brain resting state BOLD dataset into a set of spatially-structured components (Figure 1.2).

These components are typically a mixture that contains some components that represent neuronal signal and some components that represent structured noise. Therefore, ICA can be used for clean-up purposes by identifying the noise components and removing these from the data. Note that ICA can also be performed at the group-level to identify large scale resting stat. The remainder of this section focuses on using single-subject ICA for noise-reduction. When using ICA for noise-reduction, it should be applied separately to data acquired from each subject (and each run) after conventional preprocessing steps (i.e., motion correction, slice timing correction if used, temporal filtering, and spatial smoothing if used) have been applied. The output from single-subject ICA is a set of components, each of which is described by a spatial map and a timecourse. The number of components that should be extracted can be estimated automatically based on the data. Once ICA has been run to estimate the components, the next step for ICA-based cleanup is to label each of the components as either signal or noise (classification of the components). This can be done manually, based on inspecting each of the components, or the labeling can be done using one of the available automated or semi-automated ICA classification methods. Once the components have all been labeled as either signal or noise, the last step is to perform a regression analysis to remove the variance associated with the components labeled as noise from the data. There are two options for removing the noise ICA components from the data, and they are typically known as “aggressive” and “non-aggressive.” The aggressive approach is similar to nuisance regressing and removes all of the variance explained by the timeseries of the noise components from the data. This aggressive approach will lead to the

removal of all of the variance that can be explained by the timecourses, even if some of that variance is shared with signal components. The alternative, non-aggressive approach is to only remove the variance that is unique to the noise components and keep in any variance that might be related to signals of interest. That is, it keeps variance that is shared between components labeled as noise relative to components that are not clearly identifiable as being noise, and thus could contain signal. By taking into account the spatial maps and timecourses of the noise components, the regression does not fully remove all variance expressed by the noise timecourse, but only the part of the variance that is not correlated (i.e., shared) with nonnoise components. In order to preserve signal as much as possible, the "non-aggressive" approach is typically preferable, because it effectively treats signals as innocent until proven guilty

3.5 Group level ICA

ICA can be applied to data from a single subject (or run), to identify and remove noise components. However, ICA can also be used at the group level to identify large-scale resting state networks (such as the default mode network), using resting state from a group of subjects. When performing a group-ICA, the inputs are the preprocessed and cleaned resting state BOLD data from all subjects (i.e., the components extracted in the single-subject ICA decomposition are not needed for the group-ICA). To extract group-level components, it is necessary to combine the data from all subjects. Combining resting state fMRI data for a group-level ICA decomposition is typically done by spatially registering all subjects to a standard space and then temporally concatenating the registered datasets from all subjects together. This means that the dataset from

subject 2 is pasted after the last time point of the dataset from subject 1 and so on, effectively creating one very long dataset. The concatenated dataset from all subjects is then fed into ICA, and components are extracted using data from all subjects. The output from a concatenated group-ICA still contains a set of spatial maps (one per component, representing the group map), and a set of timeseries (a very long timeseries for each component, containing subject 1 first and then subject 2, etc., in order of the concatenation). Another method for running group-ICA is the tensor ICA approach, which combines all subjects in a separate subject-dimension. This approach is preferable if all subjects are expected to have similar timecourses (such as when they are all performing the same task). However, for resting state group-ICA, the temporal concatenation approach should be used. The result of a group-ICA decomposition is a single group-level spatial map for each component. However, it is often of interest to run statistical analyses to compare components between groups of subjects, for example, to ask questions like: are there any changes in the default mode network between patients suffering from depression and healthy control subjects? To address this type of question a further analysis is required to calculate subject-specific maps that can be compared, and a commonly used approach for this is a dual regression analysis, which is discussed in the next section.

3.6 Dual regression

The two stages of a dual regression analysis are essentially the same as steps two and three of an SCA (i.e., extracting the timeseries, and correlating each voxel against the extracted timeseries). In fact, if you enter a single seed-based ROI map (instead of multiple group-ICA maps)

into a dual regression analysis, the results will be identical to performing an SCA. The key difference is that we typically use a set of group-ICA maps as the input for the dual regression analysis. This means that instead of a simple correlation, we are performing multiple regression for both stage 1 and stage 2 of dual regression. Another important difference is that the group-ICA maps contain weights for all voxels, whereas a seed region in SCA is typically a binary mask (containing ones within the seed region and zeros in all other areas of the brain).

As explained in Figure 3.8, the first stage of a dual regression analysis is to perform a multiple regression analysis where the group-ICA maps are the spatial regressors (independent variables), and the subject's preprocessed BOLD dataset is the input data (dependent variable). The result of this first stage of dual regression is a set of timecourses (one for each group map) that describe the temporal structure of each component for that subject (like the timecourse extraction stage in SCA). Essentially the timecourses contain information on how much each of the components contributed to the overall BOLD signal. These timecourses derived from stage 1 of the dual regression now become the model input for the second regression. Stage 2 involves the second multiple regression analysis, where the temporal regressors obtained from stage 1 (independent variables) are regressed against the same subject's preprocessed BOLD data (dependent variable). The output of stage 2 of dual regression is a set of maps (one for each original group-level ICA component) that describe the network structure based on the data from that subject alone. Together, the outputs from stage 1 and 2 give us subject maps that best fit the group-ICA maps that are used as a starting point. The subject maps can contain either parameter estimates (beta values) or Z-statistics (which have been normalized by the within-subject noise) at every voxel. While either of these types of maps can be used for further group-level analysis, it is the

beta maps that are most commonly used. The outputs from stage 2 of the dual regression (i.e., the subject maps) are subsequently used for between-subject analyses. Specifically, the subject-specific maps can be used for group-level comparisons to study differences in network structure between subjects (which is sometimes called stage 3 of dual regression). For example, you can ask in what regions a certain network might differ in shape or strength between a group of patients and a group of healthy control subjects. Or you can look at individual difference analyses, for example, in what regions of the brain the shape or size of a network varies across subjects in a way that is linked to a cross-subject measure such as disease severity, or mathematical ability. It is important for the dual regression approach that each stage involves a multiple regression analysis. This means that regressors corresponding to all the components are entered into the model together and the best fit of each regressor is calculated while taking into account the influence of the other

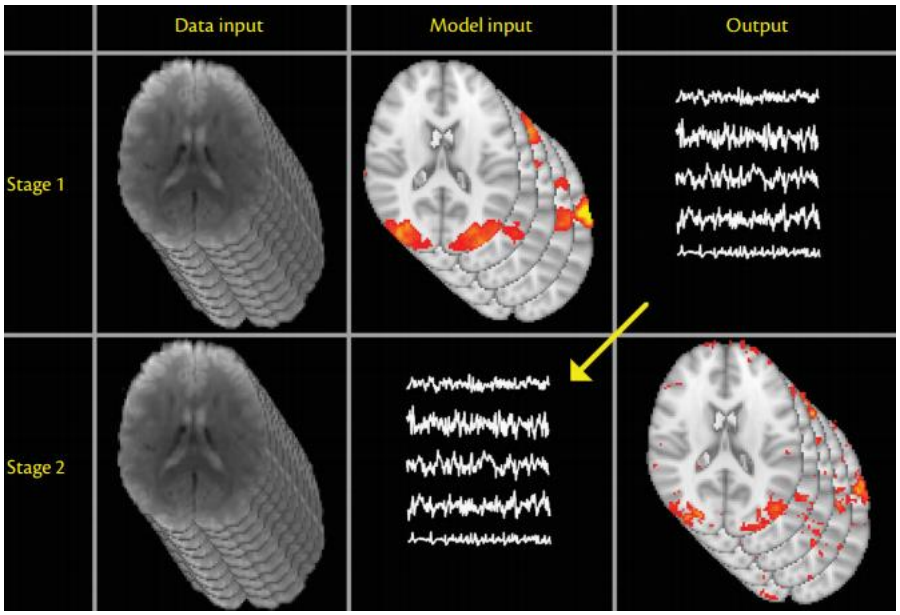

Figure 3.8: Dual regression is a two-stage process aimed at obtaining component spatial maps for every subject. The data input to the multiple regression analysis is the same in both stages (i.e., the preprocessed BOLD data from one subject). The model input for stage 1 contains the set of ICA components from the group-ICA. The outputs of stage 1 are the subject-specific component timeseries for each group component of interest, and these are used as the model input for stage 2 of the dual regression analysis. The spatial maps that are obtained from stage 2 can be used in a group analysis.

regressors. Remember that in our case the regressors for stage 1 of the dual regression represent the group-ICA maps. The set of components obtained from a group-ICA fully represent the group data (at least, the part of the group data that was kept after the PCA data reduction step). Group-ICA decomposition commonly results in multiple structured noise components even after performing careful clean-up of the subject data, because some structured noise is only detected by ICA when data from all subjects are analyzed at the same time. Therefore, the timecourses that are the output from the multiple spatial regression (stage 1 of the dual regression) represent the unique signal associated with each component, while the noise components capture confounding, unwanted noise timecourses as long as they are entered into the same multiple regression analysis. For this reason, it often is useful to include all of the components extracted from the group-ICA in the dual regression analysis, even if you are only interested in looking at a few of them in subsequent analyses. This essentially provides another useful way to denoise the single-subject estimates, by using noise components that exist on average at the group level. Further, within the dual regression procedure we go back to the full original timeseries data at both stages of the analysis.

3.7 Randomise

A common statistical problem in neuroimaging studies (that occurs in relation to null hypothesis testing) is the multiple comparisons problem (also called the multiple testing problem). In order to localize the effects of our analyses in the brain, we typically perform many tests at different locations in the brain (e.g., at each voxel). If the tests are being performed independently

(like in the SCA approach described at the start of this chapter) then this is typically referred to as a mass univariate analysis. In standard statistics, a p-value threshold of 0.05 implies that we accept a 5% chance of obtaining a false result when there is no signal. Hence, on average 1 in 20 of the tests we perform will show a significant result by chance, when there was actually no real effect there. When using a p-value threshold of 0.05 in a whole brain analysis across 20,000 voxels (i.e., we are performing 20,000 univariate tests), 5% of those, i.e., 1000 voxels in the brain will show up as being significant when there is no true effect in those voxels (they are false positives). From this example it should be clear that when we perform a large number of tests it is essential to apply some form of correction to control the number of false positives and address the multiple comparisons problem. Without appropriate correction for multiple comparisons the results of a study are highly problematic and uninterpretable because it is impossible to know which findings reflect true activation/connectivity, and which are false positives. While some studies containing uncorrected results can be found in the literature, this is poor practice that is no longer accepted by journals and reviewers. When writing up your results for publication, it is essential to specify the type of correction applied, to enable replication and to help your audience interpret the findings. In practice, the two most common approaches to multiple comparisons correction applied in neuroimaging are the family-wise error rate correction (FWE) and the false discovery rate correction (FDR). These two approaches are briefly explained here, but much more detailed information about multiple comparison correction can be found elsewhere.

n	Confidence limits for p=0.05
100	0.0500 ± 0.0436
500	0.0500 ± 0.00195
1,000	0.0500 ± 0.0138
5,000	0.0500 ± 0.0062
10,000	0.0500 ± 0.0044
50,000	0.0500 ± 0.0019

In randomise the number of permutations to use is specified with the -n option. If this number is greater than or equal to the number of possible permutations, an exhaustive test is run. If it is less than the number of possible permutations a Conditional Monte Carlo permutation test is performed. The default is 5000, though if time permits, 10000 is recommended.

4 RESULTS

Contrast 2 results shows that we have no significant difference between group A and group B Default Mode Network. The p-value selected for testing is 0.001. After selecting the p-value range, there is no number of voxels that shows significant difference. The deduced results from the comparison shows that there is no significant difference in the sensitivity of the Default Mode Network. Figure 4.1 shows the result of dual regression by applying t-test on the two groups data. The heatmap shown in this figure is the z-statistics values. In (A) we supposed that the sensitivity of default mode network in multiband factor of 4 is greater than that of Mb factor of 1. Therefore, the result shows that there is no single pixel showing significant difference. While the the other two maps are (B) and (C) are the group means of both the datasets resulted by taking independent t-test of each the dataset.

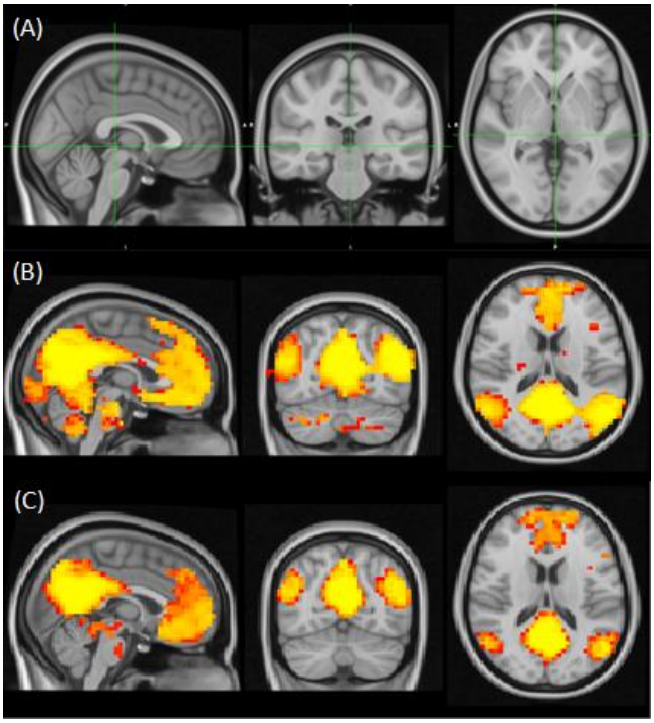

Figure 4.1: The heatmap shown in this figure is the z- statistics values. (A) is the group comparison result where there is no pixel showing significant difference. (B) map shwon in this figure is the z-values of indepandent sample t-test result. (C) map shwon in this figure is the z-values of indepandent sample t-test result.

4.1 Statistical Analysis

In addition to spatial investigation of differences in sensitivity of Default mode network further investigation was done by calculating number of voxels in each subject's DMN map. To normality of the data a well-known "Shapiro Wilk test" was applied. The p values in the graph shows that the distribution is normal, and we can do group comparison on the data.

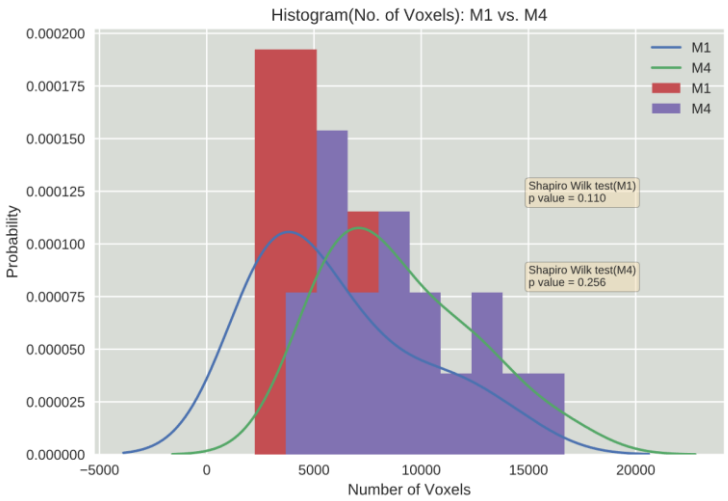

Figure 4.2: Shapiro Wilk test result, showing that the data distribution of both the groups are normal.

A two-sample independent t-test was used to check group differences. Each voxel's z-value was arranged in an array for each group. A p value of 0.001 was selected group differences investigation. Although the number of voxels in each group default mode network is different but the resulted p value shows that there is no significant difference in functional sensitivity of DMN as shown in Figure 4.3.

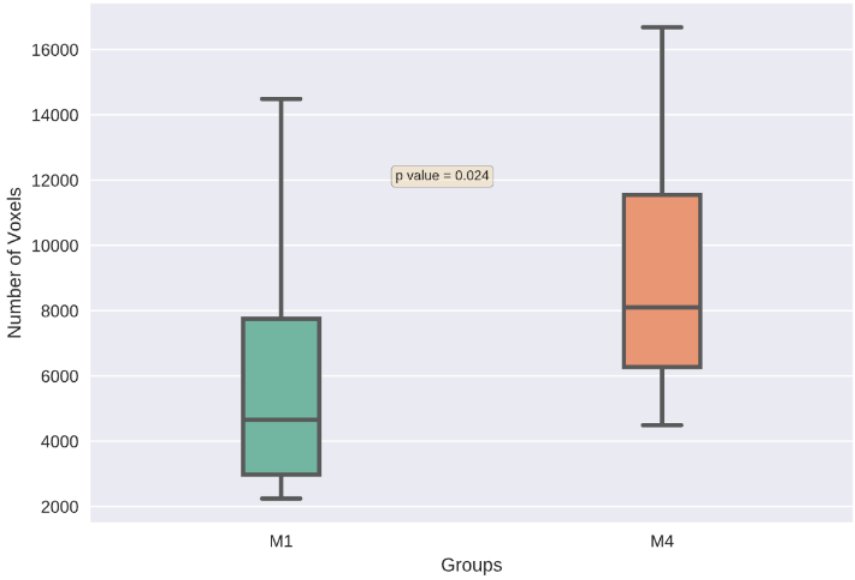

Figure 4.3: Box-plot of number of voxel in each group

References

[1]. Biswal, B., Yetkin, F.Z., Haughton, V.M., & Hyde, J.S. Functional connectivity in the motor cortex of resting human brain using echo-planar MRI. *Magnetic Resonance in Medicine.* 1995; *34*(4), 537–541.

[2]. Cole, D.M., Smith, S.M., & Beckmann, C.F. Advances and pitfalls in the analysis and interpretation of resting-state FMRI data 2010. *Frontiers in Systems Neuroscience, 4,* 8.

[3]. Larkman, David J., et al. "Use of multicoil arrays for separation of signal from multiple slices simultaneously excited." *Journal of Magnetic Resonance Imaging: An Official Journal of the International Society for Magnetic Resonance in Medicine*13.2 (2001): 313-317.

[4]. Nunes, R.G., Hajnal, J.V., Golay, X., Larkman, D.J., 2006. Simultaneous slice excitation and reconstruction for single shot EPI. Proc. Intl. Soc. Mag. Reson. Med. Seattle, Washington, USA, p. 293.

[5]. Emir, Uzay E., et al. "Regional neurochemical profiles in the human brain measured by 1H MRS at 7 T using local B1 shimming." *NMR in Biomedicine* 25.1 (2012): 152-160.

[6]. Fox MD, Raichle ME. Spontaneous fluctuations in brain activity observed with functional magnetic resonance imaging. Nat Rev Neurosci. 2007; 8(9):700–11. Epub 2007/08/21. doi: nrn2201 [pii] doi: 10.1038/nrn2201 PMID: 17704812.

[7]. Greicius M. Resting-state functional connectivity in neuropsychiatric disorders. Curr Opin Neurol. 2008; 21(4):424–30. Epub 2008/07/09. doi: 10.1097/WCO.0b013e328306f2c5 00019052-200808000-00007 [pii]. PMID: 18607202.

[8]. Mansfield P. Multi-Planar Image-Formation Using Nmr Spin Echoes. J Phys C Solid State. 1977; 10(3): L55–L8. doi: 10.1088/0022-3719/10/3/004 PMID: ISI:A1977CZ86000004.

[9]. Bandettini PA, Wong EC, Hinks RS, Tikofsky RS, Hyde JS. Time course EPI of human brain function during task activation. Magn Reson Med. 1992; 25(2):390–7. Epub 1992/06/01. PMID: 1614324.

[10]. Kwong KK, Belliveau JW, Chesler DA, Goldberg IE, Weisskoff RM, Poncelet BP, et al. Dynamic magnetic resonance imaging of human brain activity during primary sensory stimulation. Proc Natl Acad Sci U S A. 1992; 89(12):5675–9. Epub 1992/06/15. PMID: 1608978; PubMed Central PMCID: PMC49355.

[11]. Feinberg DA, Hale JD, Watts JC, Kaufman L, Mark A. Halving MR imaging time by conjugation: demonstration at 3.5 kG. Radiology. 1986; 161(2):527–31. Epub 1986/11/01. doi: 10.1148/radiology.161.2.3763926 PMID: 3763926.

[12]. Deshmane A, Gulani V, Griswold MA, Seiberlich N. Parallel MR imaging. J Magn Reson Imaging. 2012; 36(1):55–72. Epub 2012/06/15. doi: 10.1002/jmri.23639 PMID: 22696125.

[13]. Griswold MA, Jakob PM, Heidemann RM, Nittka M, Jellus V, Wang J, et al. Generalized autocalibrating partially parallel acquisitions (GRAPPA). Magn Reson Med. 2002; 47(6):120210. Epub 2002/07/12. doi: 10.1002/mrm.10171 PMID: 12111967.

[14]. Pruessmann KP, Weiger M, Scheidegger MB, Boesiger P. SENSE: sensitivity encoding for fast MRI. Magn Reson Med. 1999; 42(5):952–62. Epub 1999/11/05. doi: 10.1002/(SICI)1522-2594(199911) 42:5<952::AID-MRM16>3.0.CO;2-S [pii]. PMID: 10542355.

[15]. Liang ZP, Madore B, Glover GH, Pelc NJ. Fast algorithms for GS-model-based image reconstruction in data-sharing Fourier imaging. IEEE Trans Med Imaging. 2003; 22(8):1026–30. Epub 2003/08/09. doi: 10.1109/TMI.2003.815896 PMID: 12906256.

[16]. Tsao J, Kozerke S. MRI temporal acceleration techniques. J Magn Reson Imaging. 2012; 36(3):543–60. Epub 2012/08/21. doi: 10.1002/jmri.23640 PMID: 22903655.

[17]. van Vaals JJ, Brummer ME, Dixon WT, Tuithof HH, Engels H, Nelson RC, et al. "Keyhole" method for accelerating imaging of contrast agent uptake. J Magn Reson Imaging. 1993; 3(4):671–5. Epub 1993/ 07/01. PMID: 8347963.

[18]. Baudrexel S, Volz S, Preibisch C, Klein JC, Steinmetz H, Hilker R, et al. Rapid single-scan T2*-mapping using exponential excitation pulses and image-based correction for linear background gradients. Magn Reson Med. 2009; 62(1):263–8. Epub 2009/04/09. doi: 10.1002/mrm.21971 PMID: 19353655.

[19]. Feinberg DA, Setsompop K. Ultra-fast MRI of the human brain with simultaneous multi-slice imaging. J Magn Reson. 2013; 229:90–100. Epub 2013/03/12. doi: 10.1016/j.jmr.2013.02.002 S1090-7807(13) 00031-1 [pii]. PMID: 23473893; PubMed Central PMCID: PMC3793016.

[20]. Maudsley A. Multiple Line Scanning Spin-Density Imaging. J Comput Assist Tomo. 1981; 5(2):289–91. doi: 10.1097/00004728-198104000-00035 PMID: ISI:A1981LF71000031.

[21]. Muller S. Multifrequency selective rf pulses for multislice MR imaging. Magn Reson Med. 1988; 6(3):364–71. Epub 1988/03/01. PMID: 3362070.

[22]. Larkman DJ, Hajnal JV, Herlihy AH, Coutts GA, Young IR, Ehnholm G. Use of multicoil arrays for separation of signal from multiple slices simultaneously excited. J Magn Reson Imaging. 2001; 13(2):313–7. Epub 2001/02/13. doi: 10.1002/1522-2586(200102)13:2<313::AID-JMRI1045>3.0.CO;2-W [pii]. PMID:11169840.

[23]. Breuer FA, Kannengiesser SA, Blaimer M, Seiberlich N, Jakob PM, Griswold MA. General formulation for quantitative G-factor calculation in GRAPPA reconstructions. Magn Reson Med. 2009; 62(3):739– 46. Epub 2009/07/09. doi: 10.1002/mrm.22066 PMID: 19585608.

[24]. Nunes RG, Hajnal JV, Golay X, Larkman DJ. Simultaneous slice excitation and reconstruction for single shot EPI. Proceedings of the 14th Annual Meeting of the ISMRM, Seattle, Washington. 2006:293.

[25]. Paley MN, Lee KJ, Wild JM, Griffiths PD, Whitby EH. Simultaneous parallel inclined readout image technique. Magn Reson Imaging. 2006; 24(5):557–62. Epub 2006/06/01. doi: S0730-725X(06)00027-0 [pii] doi: 10.1016/j.mri.2005.12.019 PMID: 16735176.

[26]. Breuer FA, Blaimer M, Heidemann RM, Mueller MF, Griswold MA, Jakob PM. Controlled aliasing in parallel imaging results in higher acceleration (CAIPIRINHA) for

multi-slice imaging. Magn Reson Med. 2005; 53(3):684–91. Epub 2005/02/22. doi: 10.1002/mrm.20401 PMID: 15723404.

[27]. Setsompop K, Gagoski BA, Polimeni JR, Witzel T, Wedeen VJ, Wald LL. Blipped-controlled aliasing in parallel imaging for simultaneous multislice echo planar imaging with reduced g-factor penalty. Magn Reson Med. 2012; 67(5):1210–24. Epub 2011/08/23. doi: 10.1002/mrm.23097 PMID: 21858868; PubMed Central PMCID: PMC3323676.

[28]. Xu J, Moeller S, Auerbach EJ, Strupp J, Smith SM, Feinberg DA, et al. Evaluation of slice accelerations using multiband echo planar imaging at 3 T. Neuroimage. 2013; 83:991–1001. Epub 2013/08/01. doi:10.1016/j.neuroimage.2013.07.055 S1053-8119(13)00824-0 [pii]. PMID: 23899722; PubMed Central PMCID: PMC3815955.

[29]. Moeller S, Yacoub E, Olman CA, Auerbach E, Strupp J, Harel N, et al. Multiband multislice GE-EPI at 7 tesla, with 16-fold acceleration using partial parallel imaging with application to high spatial and temporal whole-brain fMRI. Magn Reson Med. 2010; 63(5):1144–53. Epub 2010/05/01. doi: 10.1002/mrm.22361 PMID: 20432285; PubMed Central PMCID: PMC2906244.

[30]. Feinberg DA, Moeller S, Smith SM, Auerbach E, Ramanna S, Gunther M, et al. Multiplexed echo planar imaging for sub-second whole brain FMRI and fast diffusion imaging. PLoS One. 2010; 5(12):e15710. Epub 2010/12/29. doi: 10.1371/journal.pone.0015710 PMID: 21187930; PubMed Central PMCID: PMC3004955.

[31]. Chen L, Vu A, Xu J, Moeller S, Ugurbil K, Yacoub E, et al. Evaluation of Highly Accelerated Simultaneous Multi-Slice EPI for FMRI. Neuroimage. 2014; 104C:452–9.

Epub2014/12/03. doi: S1053-8119(14)00852-0 [pii] doi: 10.1016/j.neuroimage.2014.10.027 PMID: 25462696.

[32]. Ugurbil K, Xu J, Auerbach EJ, Moeller S, Vu AT, Duarte-Carvajalino JM, et al. Pushing spatial and temporal resolution for functional and diffusion MRI in the Human Connectome Project. Neuroimage. 2013; 80:80–104. Epub 2013/05/25. doi: 10.1016/j.neuroimage.2013.05.012 S1053-8119(13)00506-5 [pii]. PMID: 23702417; PubMed Central PMCID: PMC3740184.

[33]. Boubela RN, Kalcher K, Huf W, Kronnerwetter C, Filzmoser P, Moser E. Beyond Noise: Using Temporal ICA to Extract Meaningful Information from High-Frequency fMRI Signal Fluctuations during Rest. Front Hum Neurosci. 2013; 7:168. Epub 2013/05/04. doi: 10.3389/fnhum.2013.00168 PMID: 23641208; PubMed Central PMCID: PMC3640215.

[34]. Kalcher K, Boubela RN, Huf W, Bartova L, Kronnerwetter C, Derntl B, et al. The spectral diversity of resting-state fluctuations in the human brain. PLoS One. 2014; 9(4):e93375. Epub 2014/04/15. doi: 10. 1371/journal.pone.0093375 PONE-D-13-47035 [pii]. PMID: 24728207; PubMed Central PMCID: PMC3984093.

[35]. Tong Y, Frederick BD. Studying the Spatial Distribution of Physiological Effects on BOLD Signals Using Ultrafast fMRI. Front Hum Neurosci. 2014; 8:196. Epub 2014/04/20. doi: 10.3389/fnhum.2014. 00196 PMID: 24744722; PubMed Central PMCID: PMC3978361.

[36]. Tong Y, Hocke LM, Frederick BD. Short repetition time multiband echo-planar imaging with simultaneous pulse recording allows dynamic imaging of the cardiac

pulsation signal. Magn Reson Med. 2013. Epub 2013/11/26. doi: 10.1002/mrm.25041 PMID: 24272768.

[37]. Boyacioglu R, Schulz J, Muller NC, Koopmans PJ, Barth M, Norris DG. Whole brain, high resolution multiband spin-echo EPI fMRI at 7 T: a comparison with gradient-echo EPI using a color-word Stroop task. Neuroimage. 2014; 97:142–50. Epub 2014/04/17. doi: 10.1016/j.neuroimage.2014.04.011S1053-8119(14)00266-3 [pii]. PMID: 24736172.